

New techniques to extract heat from GaN based high electron mobility transistors and LEDs

B. CHANDER JOSHI*, D. KUMAR^a, C. DHANAVANTRI

Optoelectronic Devices Group, Central Electronics Engineering Research Institute, CEERI (Council of Scientific and Industrial Research, CSIR), Pilani (Rajasthan), 333031 India

^a*Electronic Science Department, Kurukshetra University, Kurukshetra, India*

Performance of GaN based HEMTs and LEDs can be improved by using the high thermal conducting substrate materials. Still large amount of heat remain in these devices, which are sufficient to degrade the performance. By connecting metal pads to heat sink, we can improve the performance of AlGaIn/GaN HEMTs and AlGaIn/InGaIn/GaN LEDs. For HEMTs, it is observed that the source metal can extract more heat from the device, than drain contact, and in short-channel devices gate metal becomes inefficient in extracting heat from the device.

(Received April 03, 2010; accepted May 20, 2010)

Keywords: HEMT, GaN, AlGaIn, InGaIn, Contact, Substrate

1. Introduction

AlGaIn/GaN High Electron Mobility Transistor (HEMT) devices are showing remarkable performance in high speed and power applications. This is due to high breakdown field, high peak and saturation carrier velocity and good thermal conductivity demonstrated by these devices. Even without any doping a two dimensional electron gas layer (2DEG) ($n_s \sim 10^{13} \text{cm}^{-2}$) layer is formed at AlGaIn/GaN interface, due to piezoelectric and spontaneous polarizations [1]. By low temperature nucleation layer [2], annealing [3], Fe doping [4] and delta doping [5, 6], we can significantly improve the power, performance and reliability level of these devices. At present, GaN based LEDs are used for variety of applications, including traffic signals, full colour displays, back lighting in liquid crystal display and solid state lighting.

The main problem in GaN based HEMTs and LEDs is the generation of heat in the active region of the device. Failure rates in these devices are mainly determined by the operating temperature. Therefore, this is the key parameter on which the experimental/simulation studies must be focused [12]. By high thermal conducting Diamond and SiC substrate material, we can extract a lot of heat from the device [7]. Still large amount of heat remains in these

devices, which are sufficient to degrade the performance of the device. An alternate method for extracting heat from the device by thinning the substrate material [8] and substrate removal by laser lift off [9, 10, 11] is needed, to further improve the performance of these devices.

Usually in AlGaIn/GaN HEMTs source pad is connected to heat sink (by via holes and/or back side metallization), but large amount of heat is generated in between gate and drain contact. The generated heat can be conducted out by drain and gate pads more efficiently than source pads and by cathode and anode metal pads in LEDs. In this work, a novel method of heat extraction simultaneously from contacts metal pads, and effect of substrate thickness and channel length on the performance of GaN based HEMT and LED devices are studied by ATLAS.

2. Simulation approach

Monte Carlo calculated velocity and mobility at different temperatures for GaN are shown in Fig. 1. It is observed that the mobility decreases from $1020 \text{cm}^2/\text{V-s}$ to $471 \text{cm}^2/\text{V-s}$ when the temperature of device rises from 300K to 450K Table 1.

Table 1. Monte Carlo simulated electron velocity and mobility of GaN at different temperature ($n_s = 1 \times 10^{15}$).

Sl. No.	Temperature (K)	Carrier density, $\times 10^{15}(\text{cm}^{-3})$	Monte Carlo simulated mobility ($\text{cm}^2/\text{V-s}$)	Monte Carlo simulated velocity, $\times 10^7(\text{cm/s})$	Field (Maximum velocity) (kV/cm)
1	300	1	1020	2.97	154
2	400	1	604.5	2.78	164
3	500	1	376	2.59	174
4	600	1	264	2.4	184

Analytic model for mobility is formed by polynomial fit to Monte Carlo data with 10^{th} order electric field term and 2^{nd} orders temperature terms Fig. 2. Levenberg Marquat method is used for extracting the coefficient of polynomial.

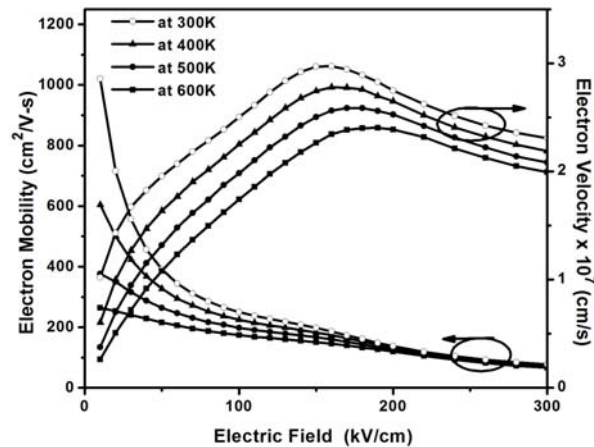


Fig. 1. Monte Carlo simulated velocity and mobility of GaN at different temperature.

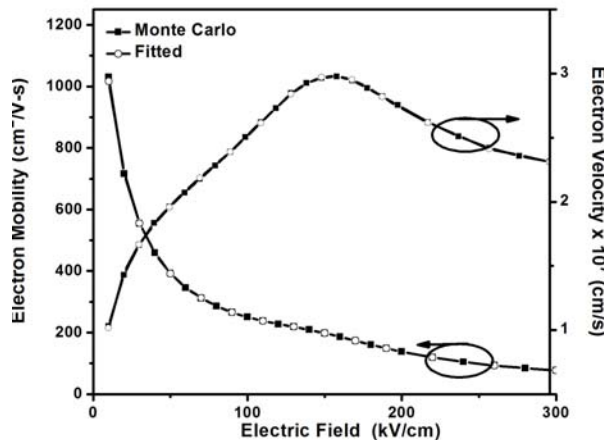
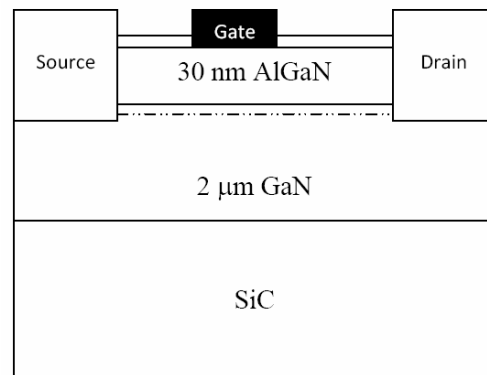
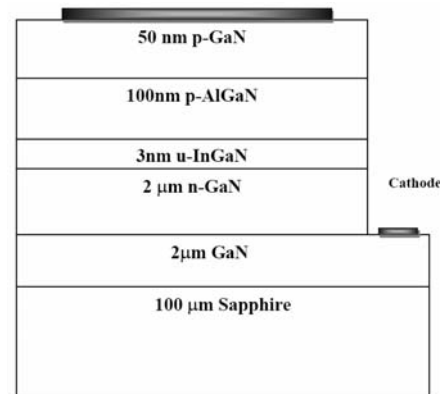


Fig. 2. Polynomial fitted and Monte Carlo simulated velocity and mobility of GaN.

GaN based HEMTs and LEDs structure used in this study are shown in Fig. 3. Gate to source and gate to drain spacing are 1 and 1.1 μm respectively for 0.7 μm (Gate length) devices and 0.25 and 0.3 μm for 0.25 μm (Gate length) devices. Detail parameters and models used in simulations are given somewhere else [7]. Atlas from M/s Silvaco is used to calculate the characteristics of these devices.



(a)



(b)

Fig. 3. (a) Schematic of AlGaIn/GaN HEMT on SiC; (b) AlGaIn/InGaIn/GaN LED on sapphire.

3. Results and discussion

Maximum channel current of 0.99 A/mm is obtained for 0.7 μm AlGaIn/GaN HEMT device on SiC. Maximum temperature of device rises to 565 K (at $V_{\text{ds}}=15$ V). When we put drain contact pads of the device to heat sink at 300K, a significant increase in performance of the device is obtained. Maximum temperature of the device falls to 464 K and maximum channel current increases to 1.58 A/mm. This improvement in the channel current gives us an idea to check the effect of metal contact pads on the performance of the device. Fig. 4 shows the variation of channel current for different thermal boundaries. Maximum channel current of 2.2 A/mm is obtained when all contact metals are thermally connected to heat sink. It is observed that, by source contact more heat is extracted from the device, then that by drain contact. Figure 5 shows the variation of device temperature with drain voltage for different thermal boundaries.

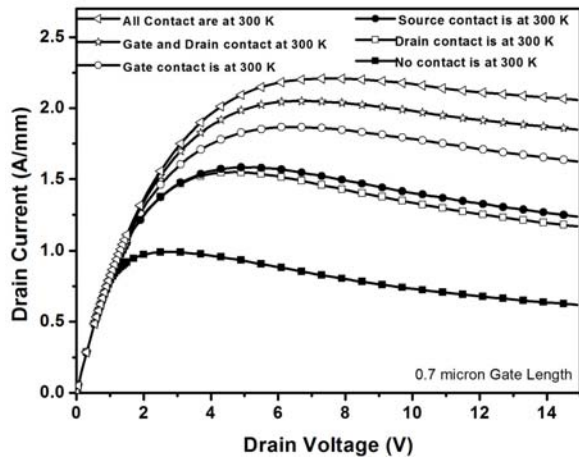


Fig. 4. I-V curves of 0.7 μm AlGaN/GaN HEMT device for different thermal boundaries.

0.7 μm AlGaN/GaN HEMT device on SiC shows maximum trans-conductance of 213 mS/mm. When drain contact is thermally connected to heat sink, trans-conductance of device increases to 268 mS/mm Fig. 5. When gate contact metal is thermally grounded, trans-conductance of device future increased to 298 mS/mm. Maximum trans-conductance (of 312 mS/mm) is obtained when all contact metals pads are thermally connected to heat sink.

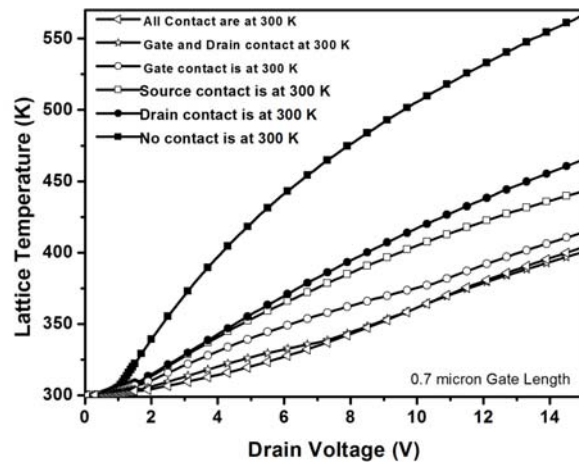


Fig. 5. Lattice temperature of 0.7 μm AlGaN/GaN HEMT device for different thermal boundaries.

Unity current gain frequency (f_t) of 0.7 μm AlGaN/GaN HEMT on SiC is 22.6 GHz. Maximum f_t of 28.7 GHz is obtained when all contact metals pads are thermally connected to heat sink Fig. cx 7.

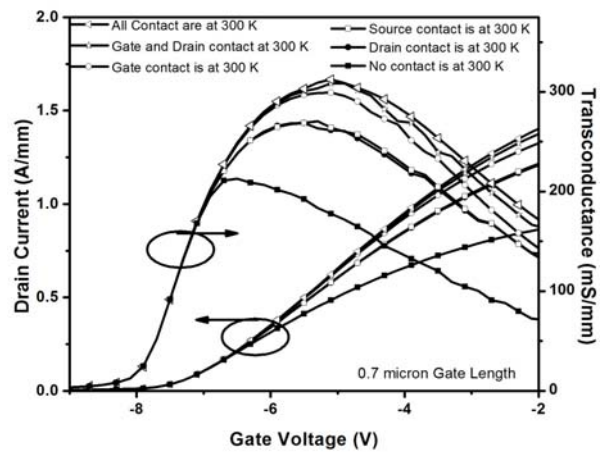


Fig. 6. Transfer and Transconductance curve of 0.7 μm AlGaN/GaN HEMT device for different thermal boundaries.

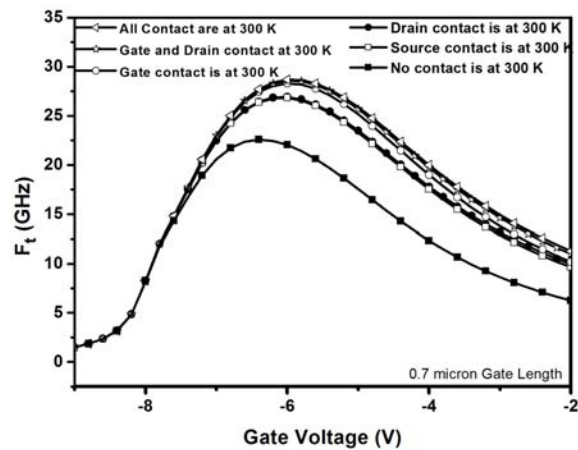


Fig. 7. f_t (unity current gain frequency) of 0.7 μm AlGaN/GaN HEMT device for different thermal boundaries.

Self heating shows a serious problem in short-channel devices. Large amount of heat is generated in short-channel devices at low drain bias. For a 0.25 μm (gate length) device maximum channel temperature rises to 600 K, when the drain is biased at 6V. Maximum channel current of 1.08 A/mm, maximum trans-conductance of 212 mS/mm and maximum f_t of 52.5 GHz is obtained for these devices. When the drain metal pads of the short-channel device is thermally connected to heat sink, maximum channel current rises to 2.56 A/mm, maximum trans-conductance rises 426 mS/mm and maximum f_t rise to 79.8 GHz. I-V and f_t curves of 0.25 μm devices for different thermal boundaries are shown in Fig. 8 and Fig. 9 respectively. It is observed that, in short-channel devices (Gate length \sim 0.25 μm) gate metal play, a very minute role in extracting heat from the device as compared to source/drain metal pads, because in short channel device, the size of gate metal pads is very less in compare to source and drain metal.

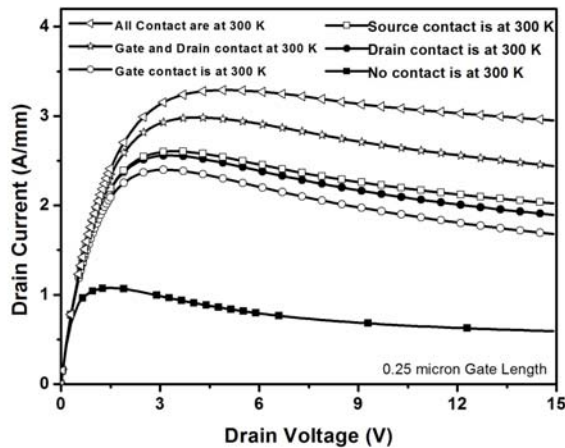


Fig. 8. I-V curves of 0.25 μm AlGaIn/GaN HEMT device for different thermal boundaries.

Effect of substrate thickness on the performance of AlGaIn/GaN HEMT is also studied. I-V and f_t curves for different substrate thickness are shown in Fig. 10 and Fig. 11, respectively.

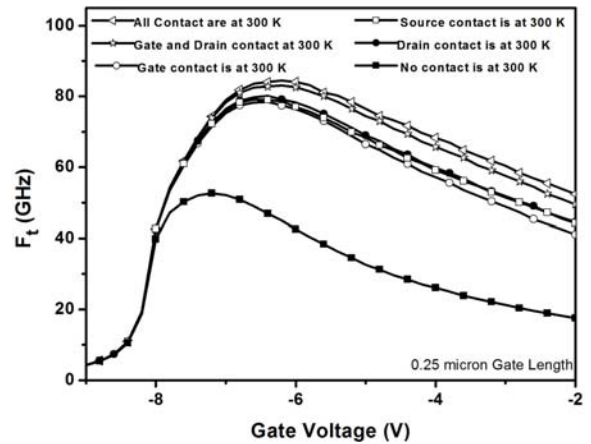


Fig. 9. f_t (unity current gain frequency) of 0.25 μm AlGaIn/GaN HEMT device for different thermal boundaries.

It is observed that in thin substrate more heat is extracted out and the performance of device increases significantly. Results extracted from different AlGaIn/GaN HEMT devices for different thermal boundaries, short-channel and substrates thickness are given in Table 2, Table 3 and Table 4 respectively.

Table 2. Results extracted from 0.7 μm AlGaIn/GaN HEMT devices for different thermal boundaries.

Thermal boundary	Gate length	Max. channel Current (mA/mm)	Channel temperature (K) at $V_{ds}=15\text{V}$	Maximum transconductance (mS/mm)	Unity current gain frequency (ft)
None	0.7	0.993	565	213	22.6
Drain Contact at 300K	0.7	1.55	442	269	26.8
Source Contact at 300K	0.7	1.59	464	271	26.8
Gate Contact at 300K	0.7	1.87	413	300	28.3
Gate Drain Contact at 300K	0.7	2.05	400	308	28.6
All Contacts are at 300K	0.7	2.2	403	313	28.7

Table 3. Results extracted from 0.25 μm AlGaIn/GaN HEMT devices for different thermal boundaries.

Thermal boundary	Gate length	Max. channel Current (mA/mm)	Channel temperature (K) at $V_{ds}=15\text{V}$	Maximum transconductance (mS/mm)	Unity current gain frequency (f)
None	0.25	1.08	868	212	52.5
Drain Contact at 300K	0.25	2.56	470	426	79.7
Source Contact at 300K	0.25	2.61	518	426	79.1
Gate Contact at 300K	0.25	2.4	510	414	78.3
Gate Drain Contact at 300K	0.25	2.98	442	464	83.2
All Contacts are at 300K	0.25	3.29	447	482	84.3

Table 4. Results extracted from 0.7 μm AlGaN/GaN HEMT devices at different substrate thickness.

Device	Substrate Thickness (μm)	Max. Channel Current (mA/mm)	Channel Temperature (K) at $V_{ds}=15V$	Maximum Transconductance (mS/mm)	Unity current gain frequency (GHz)
1	300	0.74	810	89	13.4
2	250	0.746	780	99	14.5
3	200	0.751	740	114	16.1
4	150	0.78	680	135	18.1
5	100	0.99	560	188	22.6
6	50	1.19	505	220	24.7
7	Substrate Removal	2.26	395	306	28.7

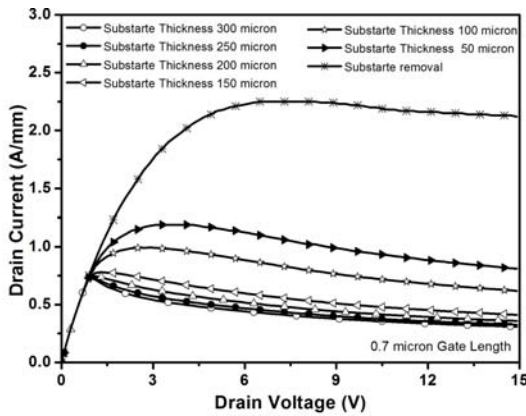


Fig.10. I-V curves of 0.7 μm AlGaN/GaN HEMT device for different substrate thickness.

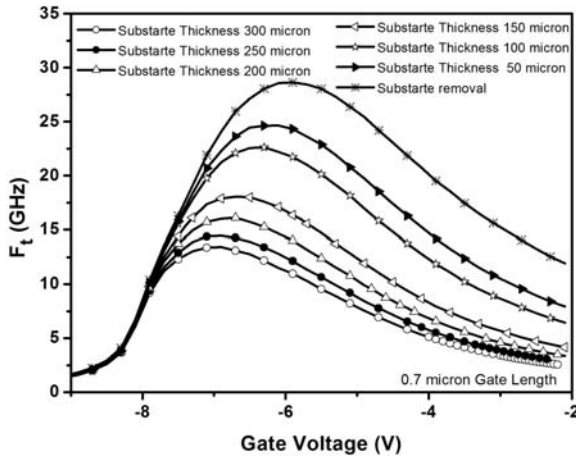


Fig.11. F_t (unity current gain frequency) of 0.7 μm AlGaN/GaN HEMT device for different substrate thickness.

In AlGaN/InGaN/GaN LED maximum temperature raises in between two contacting electrodes. Maximum temperature rises to 350K for LED structure on Sapphire at bias of 7V [8]. When we put anode contact pads of the device at 300K, maximum temperature in between two contacting electrodes of the device, falls to 316 K. Lowest

temperatures of 307 K is obtained when both of contacts pads are thermally grounded. Variations of temperature of device with anode voltage for different thermal grounding scheme are shown in Fig. 12. I-V curves for different thermal grounding scheme are shown in Fig. 13.

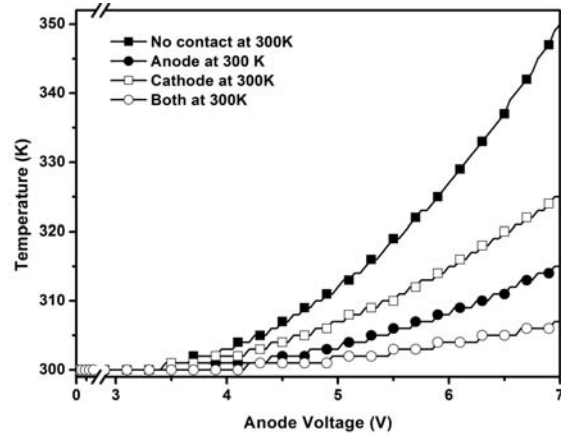


Fig.12. LED device temperature with respect to Anode Voltage for different thermal grounding scheme.

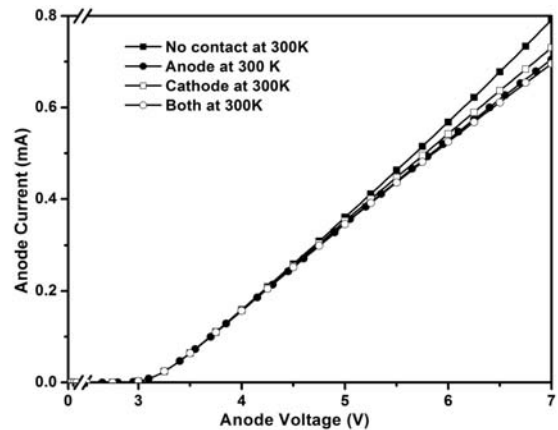


Fig.13. I-V Curves for AlGaN/InGaN/GaN LED for different thermal grounding scheme.

Large amount heat is generated in multi Quantum well (QW), and multi finger LED structures. Double QW LED structures on Sapphire are studied by ATLAS. Maximum temperature of 345 K is obtained at anode biased at 7V. When all contacts metal pads are thermally grounded the maximum temperature in between two contacts, reduces to 305 K. EL curve for single and double QW LEDs structures are shown in Fig. 14. In multi fingered design LEDs, maximum temperature of device rises to 364K, when all contacts metals pads are thermally grounded the maximum temperature in device falls to 315K. Fig. 15 shows device temperature versus anode bias for double QW design and multi fingers design LEDs structures.

Fig. 16 shows the effect of substrate thickness on device operational temperature. It is observed that maximum heat from all of these devices is extracted by thermal grounding all the contacts metal pads or/and by thinning the substrate materials. Table 5 shows the results extracted from different LEDs structures.

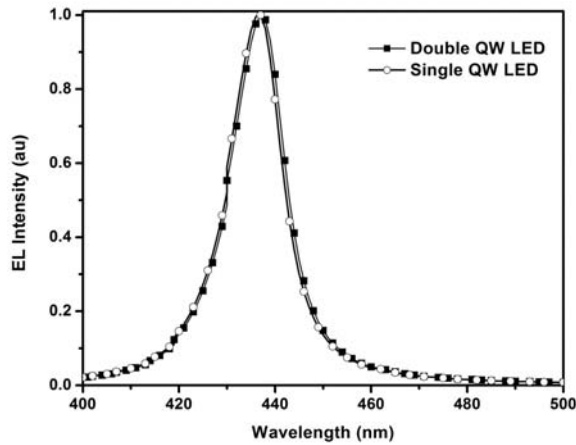


Fig.14. EL curve for single and double quantum well LEDs.

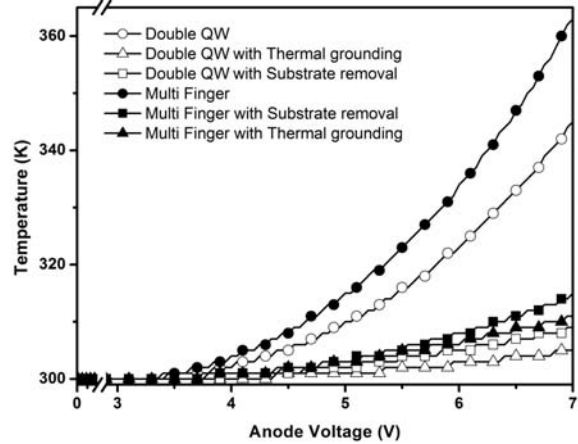


Fig.15. LED device temperature with respect to Anode Voltage for double QW and multi fingers design LEDs structures.

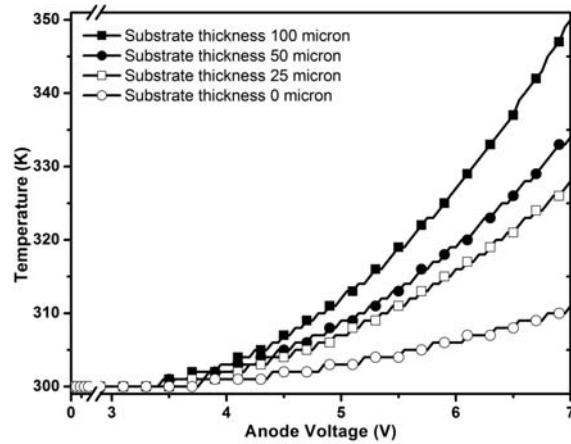


Fig.16. LED device temperature with respect to Anode Voltage for different substrates thicknesses.

Table 5. Results from different LEDs structures.

No. of Quantum well	Multi fingered device	Anode at 300K	Cathode at 300K	Substrate thickness (μm)	Temperature (K) at $V_{anode}=7V$	Anode Current (mA) at $V_{anode}=7V$	EL peak intensity (nm)
1	No	No	No	100	350	800	437
1	No	Yes	No	100	316	706	437
1	No	No	Yes	100	325	735	437
1	No	Yes	Yes	100	307	700	437
2	No	No	No	100	345	707	437.1
2	No	Yes	Yes	100	305	584	437.1
2	No	No	No	0	309	596	437.1
1	Yes	No	No	100	364	1620	437
1	Yes	Yes	Yes	100	315	1374	437
1	Yes	No	No	0	311	1379	437
1	No	No	No	50	334	756	437
1	No	No	No	25	328	741	437
1	No	No	No	0	311	702	437

4. Conclusions

High thermal conducting substrate materials extract lots of heat from the device, but in AlGaIn/GaN HEMTs, the temperature of the device in the channel at the gate-drain edge is still sufficient to cause mobility degradation and thus degrade the performance of the device. In AlGaIn/InGaIn/GaN LED maximum temperature rises in between two contacting metals. When contacting metals of these devices are thermally grounded, a noticeable improvement in the performance is observed. Improvement in performance of the device, directly correlate with the large extraction of heat from these devices. In short-channel HEMTs, gate metal plays a very little role in comparison to source and drain metals in extracting heat from the device. Large amount of heat is generated in multi finger and multi quantum well LEDs structure, which can easily extracted by thinning the substrates material and/or by thermal grounding the contacts metals pads. By optimizing the device geometry, we can further extract heat and drastically improve the performance level of these devices.

Acknowledgements

The authors would like to thanks the Director of Central Electronics Engineering Research Institute (CEERI), Pilani, Rajasthan, India, for his encouragement, and concerned members of the Optoelectronic Devices Group and Semiconductor Device Fabrication Facility, CEERI, for their help at various stages. One of the authors Bhubesh Chander Joshi acknowledges CSIR, New Delhi for SRF.

References

- [1] J. P. Ibbeton, P. T. Fini, K. D. Ness, S. P. DenBaars, J. S. Speck, U. K. Mishra, *Applied Physics Letter* **77**, 250 (2000).
- [2] Akasaki, H. Amano, Y. Koide, K. Hiramatsu, N. Sawaki, *Journal of Crystal Growth* **98**, 209 (1989).
- [3] C. F. Lin, G. C. Chi, M. S. Feng, J. D. Guo, J. T. Tsang, J. M. Hong, *Applied Physics Letter* **68**, 3758 (1996).
- [4] C. C. Young, C. Ho-Young, G. Spencer Michael, F. Eastman Lester, *IEEE Transactions on Electron Devices* **53**, 2926 (2006).
- [5] B. C. Joshi, N. Pradhan, M. Mathew, K. Singh, C. Dhanavantri, D. Kumar, *Optoelectron. Adv. Mater.- Rapid Comm.* **3**(10), 985 (2009)
- [6] H. Lahre Che, P. Venne Gue, B. Beaumont, P. Gibart, *Journal of Crystal Growth* **205**, 245 (1999).
- [7] B. C. Joshi, C. Dhanavanti, D. Kumar, J. *Optoelectron. Adv. Mater.* **11**, 1111 (2009).
- [8] Y. Ando, Y. Okamoto, H. Miyamoto, N. Hayama, T. Nakayama, K. Kasahara, M. Kuzuhara, *IEDM Tech. Dig.*, **17**(3), 1 (2001).
- [9] J. G. Felbinger, M. V. S. Chandra, Y. Sun, Lester F. Eastman, J. Wasserbauer, F. Faili, D. Babic, D. Francis, F. Ejeckam, *IEEE Electron Device Letters* **28**, 948 (2007).
- [10] J. Das, W. Ruythooren, R. Vandersmissen, J. Derluyn, M. Germain, G. Borghs, *Phys. Status Solidi. (c)* **2**, 2655 (2005).
- [11] E. Yablonovitch, D. Hwang, T. Gmitter, L. Florez, J. Harbison, *Applied Physics Letter* **56**, 2419 (1990).
- [12] P. Regoliosi, A. Reale, A. Di Carlo, P. Romanini, M. Peroni, C. Lanzieri, A. Angelini, M. Pirola, G. Ghione, *IEEE Transactions On Electron Devices* **53**, 182 (2006).

*Corresponding author: bhubesh25@gmail.com